CORE
Metadata, citation and similar papers at core.ac.uk
Provided by Digital.CSIC

Morphological and magnetic properties of Co nanoparticle thin films grown on Si_3N_4

B. Presa[a] and R. Matarranz
Departamento de Física, Facultad de Ciencias, Universidad de Oviedo, Calvo Sotelo S/N, 33007 Oviedo, Spain

C. Clavero and J. M. García-Martín
Instituto de Microelectrónica de Madrid-IMM (CNM-CSIC), Isaac Newton 8 (PTM), 28760 Tres Cantos, Madrid, Spain

J. F. Calleja and M. C. Contreras
Departamento de Física, Facultad de Ciencias, Universidad de Oviedo, Calvo Sotelo S/N, 33007 Oviedo, Spain

(Received 6 February 2007; accepted 14 July 2007; published online 4 September 2007)

The morphological and magnetic properties of Co nanoparticles deposited by triode sputtering on Si_3N_4 at 550 °C are reported. The nominal thickness of Co ranges from 2 up to 15 nm, and two different capping layers, Au and Pt, are used. The nanoparticles were characterized by x-ray diffraction and atomic force microscopy. Morphological and structural studies show that the nanoparticles grow in a well-defined nanostructured pattern and adopt a hexagonal closed packed crystalline structure. Moreover, the average particle size and the particle size dispersion increase as the thickness increases, due to percolation. Experimental characterization of effective anisotropy field was carried out with transverse susceptibility. Transverse susceptibility measurements reveal an in-plane isotropic magnetic behavior. Both the effective anisotropy field and the coercive field increase as the particle size increases, following a D^6 dependence, which is typical for three-dimensional structures in the framework of the random anisotropy model. The relationship between the particle size distribution and the anisotropy field distribution is shown, explaining the significant dependence of the magnetic behavior on the Co layer thickness. On the other hand, different capping layers give rise to a change in the magnetic response due to the modification of the interparticle interaction. © *2007 American Institute of Physics*. [DOI: 10.1063/1.2775172]

I. INTRODUCTION

One of the most interesting problems in modern condensed matter physics is the study of nanostructures, especially magnetic low-dimensional systems. In such systems, structural properties (crystallographic structure, particle size, and texture) deeply affect magnetic properties such as anisotropy, coercivity, and magnetization reversal process. Research on these systems has led to the development of new technological applications such as ultrahigh-density computer disk drives[1,2] and magnetic sensors.[3,4] For example, Co nanoparticles,[5,6] Co nanocolumns,[7] and Co-based alloys[8] have attracted a lot of attention in the past decade since they may be good candidates for high-density storage media. A critical feature is the reduced particle size which causes thermal relaxation of magnetic moments[9] and a modification of the effective anisotropy through interparticle interaction.[10]

Measurement of the transverse susceptibility (χ_T) at room temperature has proven to be a very powerful technique to obtain the effective anisotropy field, the interparticle interaction, texture, and anisotropy field distribution in nanostructured systems.[11–13] The value of the effective anisotropy field depends on several parameters such as the intrinsic anisotropy constant K_1 of the particles, their volume V, and the temperature T that produces the thermal fluctuations. The activation energy required to reverse the particle's magnetization is given by K_1V. Therefore, if k_BT is not small enough compared to K_1V, the period of stability of the particle's magnetization will not be long enough for the particle to be used as a magnetic bit. Then the system is said to be superparamagnetic. Lowering the superparamagnetic limit requires new ways of enhancing the anisotropy of the magnetic bits.

Recently, Spinu *et al.*[14,15] have pointed out the influence of temperature in the χ_T response of nanoparticle systems, distinguishing between the blocked and superparamagnetic states for fixed activation energy. Nevertheless, another interesting point of view for this problem is to change the activation energy of the particles, varying their volumes or even changing the capping layer, for fixed temperature, as it is well known that the capping layer can produce an enhancement of the magnetic anisotropy due to interparticle interaction.[16] In this work, two different capping layers, Au and Pt, are used. Pt polarization has been widely studied by means of x-ray magnetic circular dichroism (XMCD),[17] Kerr spectroscopy,[18,19] and *ab initio* simulations in Co/Pt interfaces and multilayers. In all the cases, the polarization of the Pt atoms has been observed when they make contact with a Co surface, due to orbital hybridization between Co 3*d* and Pt 5*d*, giving rise to a perpendicular magnetic anisotropy in

[a]Electronic mail: presaborja.uo@uniovi.es

 © 2007 American Institute of Physics

Downloaded 28 Apr 2009 to 161.111.235.57. Redistribution subject to AIP license or copyright; see http://jap.aip.org/jap/copyright.jsp

the Co/Pt interface. Suzuki *et al.*[17] observed a total magnetic moment of 0.61 μ_B/atom for the Pt atoms at the interface and an exponential decrease of the magnetic moment from the interface. The polarization of the Au atoms has also been studied when they make contact with a Co surface.[20] In this case, the induced magnetic moment of Au was very small, about one order of magnitude smaller than that of Pt.

The present paper is focused on the magnetic properties of $Co/Si_3N_4/Si(100)$ thin films. Both the role of Co nanoparticle size and the influence of the kind of capping layer used are investigated. In order to characterize the physical properties of the Co nanoparticles, x-ray diffraction (XRD) and atomic force microscopy (AFM) were used. The correlation between morphology, especially the mean particle size and the particle size dispersion, and the magnetic properties is discussed.

II. EXPERIMENT

The samples were grown in an ultrahigh vacuum multichamber with triode sputtering facility (base pressure about 10^{-9} mbar, work pressure $P_{Ar}=4\times10^{-4}$ mbar, and deposition rates 0.50, 0.37, and 0.30 Å/s for Au, Co, and Pt, respectively). Co deposition was performed at 550 °C in order to favor the formation of nanoparticles. Si(100) substrates covered with a 100-nm-thick Si_3N_4 buffer layer were used. A 2-nm-thick capping layer was grown by sputtering, at room temperature, to obtain a conformal growing. The capping layer material was chosen to be a low polarizable material (Au) or a highly polarizable one (Pt). Particle size and physical contact between them were controlled by deposition time and studied with AFM. Particle size in the film plane was obtained for all samples by measuring and counting the particles' diameter using a Zeiss particle size analyzer. More details regarding particle size analysis can be found elsewhere.[21] Roughness analysis of the samples was done with the free commercial program WSXM.[22]

The magnetic properties of the samples were obtained from χ_T measurements performed by a transverse magneto-optical Kerr effect. This basically consists of the application of a small alternating magnetic field H_1 and an orthogonal steady field H, both in the film plane, as can be seen in Fig. 1. The Kerr signal is proportional to the component of the magnetization parallel to H_1 (ΔM). If the amplitude of H_1 is small enough, ΔM is proportional to the susceptibility, and then this magnitude, in a direction parallel to H_1, is measured as a function of H. In our case, H_1 had a frequency of 127 Hz. The same experimental setup was used to obtain the magneto-optical transverse Kerr hysteresis loops of the samples. Also polar Kerr spectra were acquired with a maximum field of 1.6 T applied in the perpendicular direction.

III. RESULTS AND DISCUSSION

A. Morphological and structural properties

AFM results for the Au and Pt capped samples are shown in Figs. 2 and 3, respectively. The particle size distribution was fitted to a log-normal distribution. *Ex situ* AFM measurements were performed in capped samples and reveal a well-defined nanostructured pattern without any coalescence for the thinner Co layers. This real space microscopic characterization technique allowed us to get direct evidence of the three-dimensional (3D) growth for these structures: uncovered substrate areas were observed and therefore excess of material accumulated on top of the particles. For low coverage, Co aggregates into small nanoparticles that increase their size and percolate with increasing deposition time. The mean particle size (D) ranges from 12.5 up to 84.1 nm and the mean roughness (H) ranges from 1.0 up to 10.8 nm. H is the mean value of the vertical distance covered by the tip in the AFM measurements. The values of D, H, and the corresponding standard deviations (σ_D and σ_H) are displayed in Table I. The nominal thickness of Co (t_{Co}) corresponds to that of a continuous and flat Co film if grown on the same substrate but at lower temperature [giving rise to two-dimensional (2D) growth]. Since a 2-nm-thick capping layer covers the nanoparticles, H does not correspond exactly to the mean nanoparticle height. It is worth pointing out that the behaviors of D and H are different: while D increases

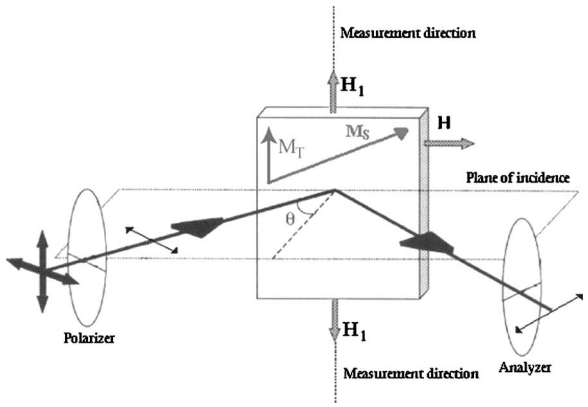

FIG. 1. Schematic diagram of the magneto-optical experimental setup used for the measurement of the transverse susceptibility and the hysteresis loops. The transverse component of the magnetization M_T is measured as a function of H_1 (hysteresis loop) or as a function of H (transverse susceptibility).

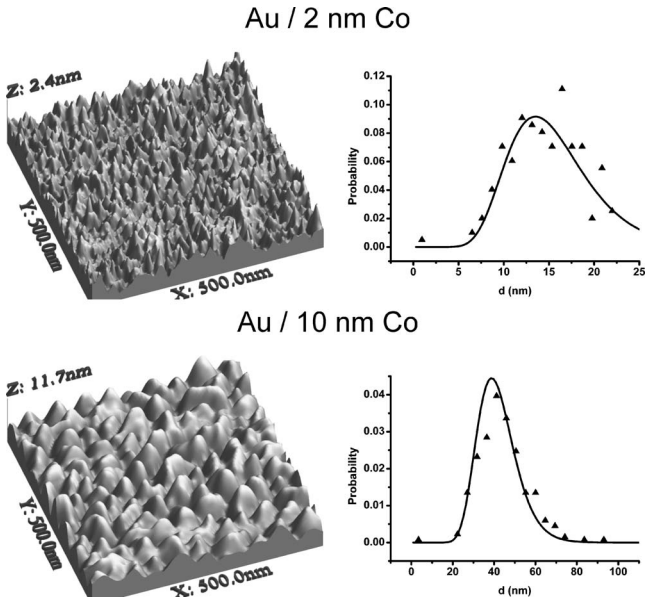

FIG. 2. 3D AFM images and nanoparticle size distributions of Au capped samples with different Co nominal thicknesses.

Downloaded 28 Apr 2009 to 161.111.235.57. Redistribution subject to AIP license or copyright; see http://jap.aip.org/jap/copyright.jsp

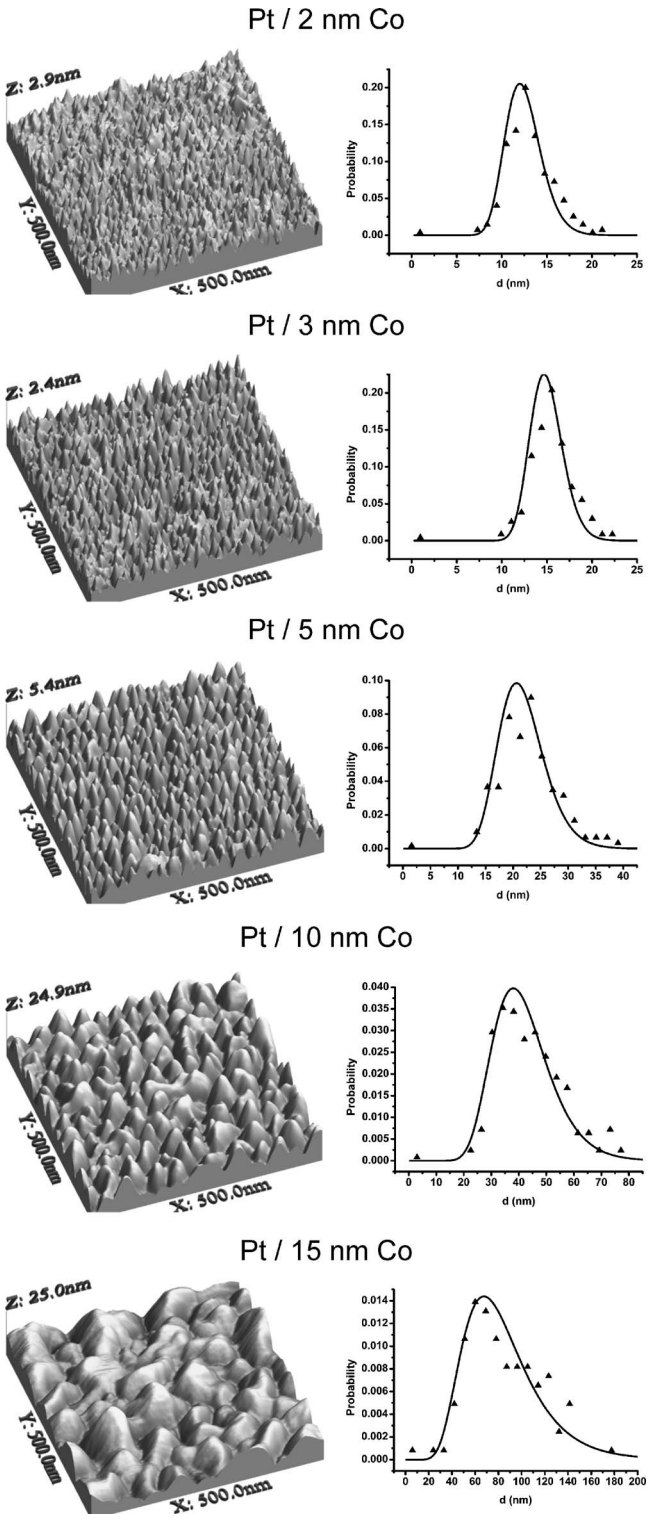

FIG. 3. 3D AFM images and nanoparticle size distributions of Pt capped samples with different Co nominal thicknesses.

with increasing amounts of Co, as expected, H reaches a maximum for 10-nm-thick Co layer. This is due to the fact that when the deposition time is increased, the nanoparticles grow completely, filling up the substrate (see Figs. 2 and 3). Similar features are obtained with the corresponding standard deviations: while σ_D increases due to the percolation between nanoparticles, σ_H reaches a maximum with increasing Co thickness. Moreover, the results of the analysis of the AFM images show that D and σ_D are always greater than H and σ_H, respectively. The samples with smaller nanoparticles show a homogeneous size distribution; this implies a narrower anisotropy field distribution, as will be shown in the next section. On the other hand, a slight difference in the morphological results is obtained between the two capping layers. It is worth noting that the Au capped thin film with a Co nominal thickness of 10 nm shows less roughness than the Pt capped one (see the reduction of both H and σ_H in Table I). It seems that platinum tends to cover the top of the nanoparticles, whereas gold may enter deeper between them. This might be due to the different surface diffusion of Au and Pt atoms in Co.

TABLE I. Co nominal thickness (t_{Co}), mean particle size (D), mean roughness (H), and the corresponding standard deviations (σ_D and σ_H) for Co nanoparticle thin films.

Capping layer	t_{Co} (nm)	D (nm)	σ_D (nm)	H (nm)	σ_H (nm)
Au	2	15.6	4.9	1.0	0.3
	10	41.8	9.6	5.2	1.6
Pt	2	12.5	2.0	1.4	0.3
	3	15.0	1.8	1.1	0.3
	5	21.8	4.2	2.4	0.8
	10	41.9	10.9	10.8	3.8
	15	84.1	33.3	9.5	3.7

Ex situ XRD measurements show that Co mainly crystallizes in its hexagonal metallic phase without texture since the $(10\bar{1}0)$, (0002), and $(10\bar{1}1)$ hcp Co diffraction peaks are observed for thicknesses down to 5 nm. As expected, the intensity and width of these peaks evolve with the Co nominal thickness, being more intense and narrower for the thicker samples. This reveals an increase of the grain size, in agreement with other similar systems.[23]

B. Magnetic properties

The magnetic properties of the samples were investigated by measuring polar Kerr loops, transverse Kerr loops, and χ_T at room temperature. These techniques allow us to have a complete characterization of the magnetic process either in the film plane or out of plane. In the case of polar Kerr loops, the magnetic field $H_\perp$ is applied perpendicular to the film plane and the Kerr rotation angle of the light is measured. This Kerr rotation is proportional to the magnetization parallel to $H_\perp$. The resulting hysteresis loops are displayed in Fig. 4. Loops with a low remanence and coercive field are found in all the samples, typical of a system with in-plane magnetization. However, the effect of the Co nominal thickness is present in the measurements. A gradual increase of the saturation field can be seen in Fig. 4, corresponding to the transition from a system with small magnetically isolated nanoparticles to a percolated system with large aggregates (as observed by AFM). Consequently, the magnetic size of the nanoparticles in the direction perpendicular to the substrate plane exerts influence on the effective anisotropy energy out of plane. On the contrary, the capping layer has only a slight influence on the magnetization process. The saturation field of the Pt capped samples seems to be slightly lower than that of Au capped ones, prob-

Downloaded 28 Apr 2009 to 161.111.235.57. Redistribution subject to AIP license or copyright; see http://jap.aip.org/jap/copyright.jsp

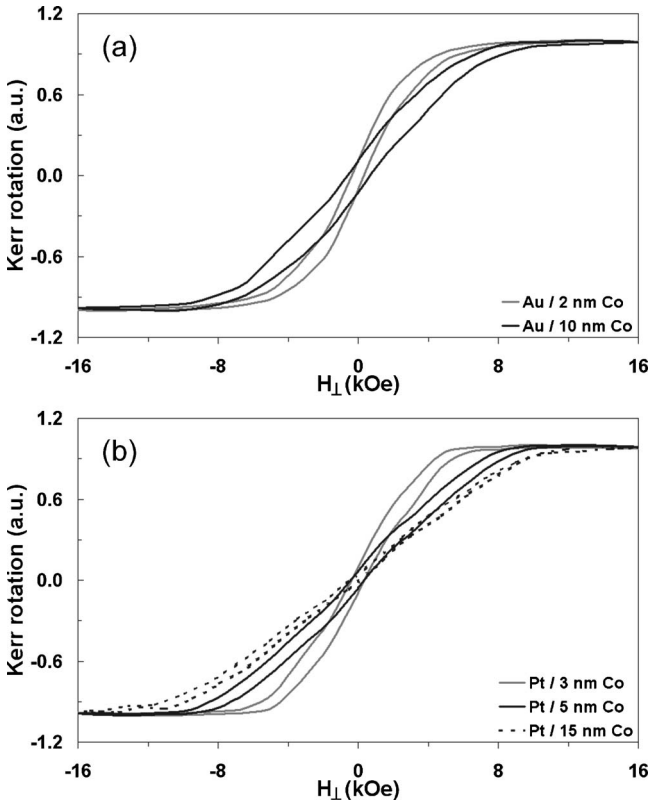

FIG. 4. (a) Hysteresis loops measured in the polar Kerr configuration for Au capped samples with Co nominal thicknesses of 2 and 10 nm. (b) Hysteresis loops measured in the polar Kerr configuration for Pt capped samples with Co nominal thicknesses of 3, 5, and 15 nm.

ably due to the formation of perpendicular anisotropy in the Co/Pt interface.[18] However, the capping layer has much more influence in the in-plane magnetization process as will be shown later on.

In order to investigate the in-plane magnetization, transverse Kerr hysteresis loops were measured for all the samples along several directions. Isotropic magnetic behaviors were obtained, i.e., the shape of the hysteresis loop does not depend on the direction in which the magnetic field H_1 is applied. Therefore, there is a lack of easy and hard magnetization axes. This is related to the fact that Co nanoparticles, grown on an amorphous buffer layer (Si_3N_4) at 550 °C, form a randomly oriented system. Figure 5(a) displays the transverse Kerr hysteresis loops for the samples with Au capping layer. The results for the samples with Pt capping layer can be seen in Fig. 5(b). Unfortunately, in this case, it was not possible to saturate the samples with nominal thicknesses of 10 and 15 nm in our experimental setup, observing only the Rayleigh region. The coercivity data have been included in Table II.

In the case of Au capped samples [see Fig. 5(a)], there are rotations involved in the magnetization reversal. Moreover, the hysteresis loop of the sample with a Co nominal thickness of 2 nm shows a behavior close to a superparamagnetic state. Let us consider, in a rough approximation, the nanoparticles in the shape of an oblate spheroid, $D/2$ being its major axis and $(H+t_{Co})/2$ its minor axis. In this case, the volume of a particle is given by $\pi D^2(H+t_{Co})/6$. The values of $\alpha(=K_1V/k_BT)$ at room temperature are included in Table II

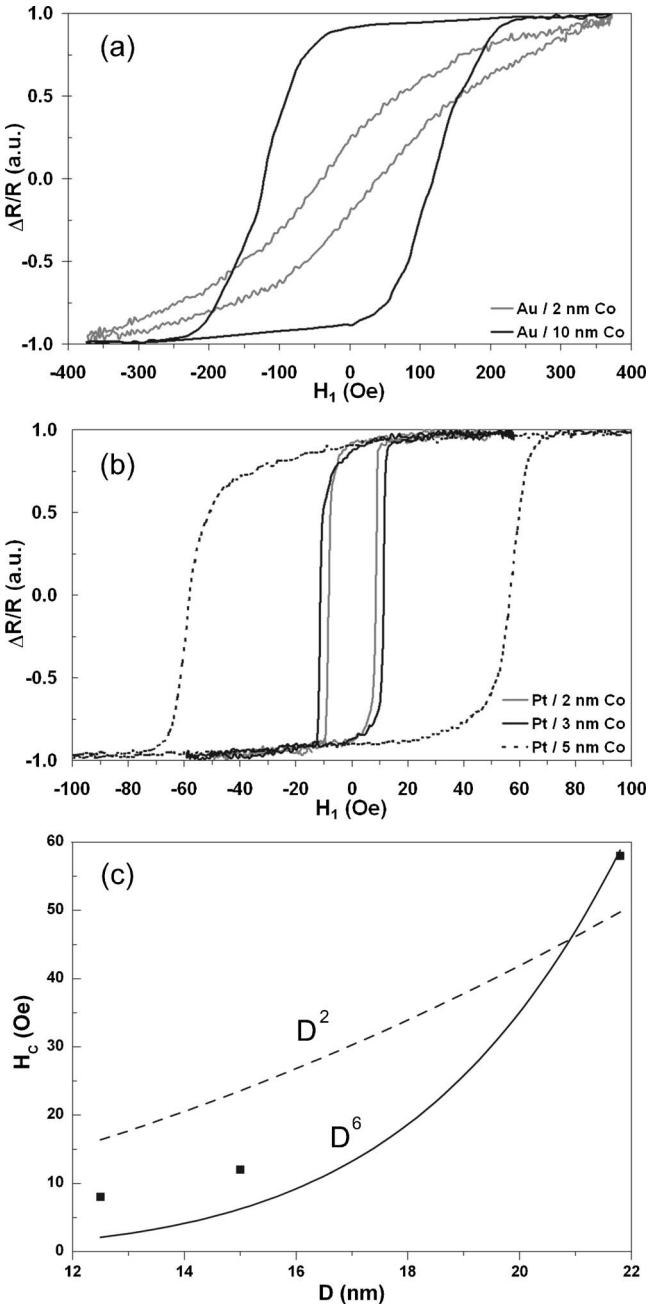

FIG. 5. (a) Hysteresis loops measured in the transverse Kerr configuration for Au capped samples with Co nominal thicknesses of 2 and 10 nm. (b) Hysteresis loops measured in the transverse Kerr configuration for Pt capped samples with Co nominal thicknesses of 2, 3, and 5 nm. (c) Dependence of Pt capped Co nanoparticles' coercivity on particle size with the corresponding fits to D^6 law (solid line) and D^2 law (dashed line).

for each nanoparticulated sample, K_1 being the magnetic anisotropy constant[24] of bulk Co ($K_1=4.1\times10^5$ J/m^3). This ratio between the activation and thermal energies allows us to determine the transition from one equilibrium state to the other. For example, the medium thermal stability criterion is given by $\alpha\geq60$, which defines a thermally stable state for a ten year period.[25] In our case, the α values are low for the thinner samples. This is the reason why the Au capped sample with a Co nominal thickness of 2 nm has a high superparamagnetic component. However, when the particle size increases, a ferromagnetic behavior is observed [see Fig. 5(a)], as expected. Magnetization rotations are involved in

Downloaded 28 Apr 2009 to 161.111.235.57. Redistribution subject to AIP license or copyright; see http://jap.aip.org/jap/copyright.jsp

the magnetization reversal of the Au capped sample with a Co nominal thickness of 10 nm. It also exhibits a high coercivity, typical of a ferromagnetic state.

On the other hand, the Pt capping layer has a drastic effect on the magnetic properties of the Co nanoparticles, as can be seen in Fig. 5(b). Even the thinner samples show a clear ferromagnetic behavior. This is due to the different polarizability of Au and Pt. Hence, while the nanoparticles of Pt capped samples are magnetically connected via the capping, the nanoparticles of Au capped samples must be disconnected. When Pt is used, an increase of the effective magnetic volume of the particles is promoted and so it is easier to overcome the thermal instability. When the particle size increases, the magnetization reversal becomes more complicated, involving more rotations, showing a sharp increase in the coercivity [see Fig. 5(b)]. For low Co nominal thickness, the effective anisotropy is small and soft magnetism is observed due to a scaling down of the local anisotropy. However, when the particle size increases, the magnetization vector is more strongly constrained by the orientation of the local anisotropy and saturation of the magnetization is harder to achieve. The magnetic anisotropy in polycrystalline ferromagnetic films is well described by the random anisotropy model (RAM). According to this model,[26] when the particle size is smaller than the exchange length, the effective anisotropy energy K_{eff} variation with the particle size follows $D^{2/3}$, D^2, and D^6 laws for one-dimensional, two-dimensional, and three-dimensional structures, respectively. Moreover, in this framework, the coercivity is proportional to K_{eff}. In Fig. 5(c) we have plotted H_C vs D for the samples with $t_{\text{Co}}=2$, 3, and 5 nm, with Pt capping layer. The corresponding fits to D^2 (dashed line) and D^6 (solid line) laws have been applied to the experimental data, which are closer to D^6 dependence. Although Co nanoparticles always have a mean particle size bigger than the mean height, the ratio between D and H is around 10, yielding a growth mode closer to three dimensions. This behavior of H_C is completely different from that which can be obtained when the deposition is performed at room temperature. In such a case, a continuous thin film growth is promoted. For example, Kharmouche *et al.*[27] achieved a constant coercivity around 10 Oe for a wide range of thickness in Co films deposited at room temperature on glass, which is another amorphous substrate.

We now turn to the χ_T measurements, which provide a fairly accurate description of the magnetic anisotropies involved in a system and a picture of the magnetization reversal mechanism along the direction in which the steady field H is applied. Let us keep in mind that while the transverse hysteresis loop is a representation of M_T vs H_1, χ_T is a representation of dM_T/dH_1 vs H. Accordingly, any small change in the component of the magnetization along H induces a small change in M_T, which can be detected as a peak in the dM_T/dH_1. This response makes χ_T a very sensitive technique to detect the magnetic anisotropy in a nanoparticulated system. In the case of noninteracting uniaxial randomly oriented single-domain particle systems, the Stoner-Wohlfarth model predicts characteristic peaks in the field dependence of the χ_T located at $\pm H_K$ and $-H_C$.[28]. Pareti and Turilli[29] provided the first experimental confirmation in polycrystalline samples of $BaFe_{12}O_{19}$. However, the effect of interparticle interaction, anisotropy field dispersion, and texture complicates the behavior of these systems.[11,13,30–33]

TABLE II. Co nominal thickness (t_{Co}), coercivity (H_C), effective anisotropy field ($H_{K,\text{eff}}$), and the parameter α ($=K_1V/k_BT$) at room temperature for Co nanoparticle thin films.

Capping layer	t_{Co} (nm)	H_C (Oe)	$H_{K,\text{eff}}$ (Oe)	α
Au	2	35	⋯	38
	10	120	200	1380
Pt	2	8	10	28
	3	12	21	47
	5	58	77	183

According to the experimental χ_T curves, all the samples exhibit a magnetic isotropic behavior, i.e., the shape of the χ_T curve does not depend on the direction in which the steady field H is applied. The χ_T was always measured from positive to negative saturation. In Fig. 6(a) we have displayed the χ_T measurements for Au capped samples. The most characteristic feature of the χ_T curve for the Au capped sample with $t_{\text{Co}}=2$ nm is that it has only one rounded peak located at $H=0$. Moreover, let us remember that the transverse Kerr hysteresis loop for this sample was close to an S shape. Similar results have been obtained by other authors[14,34,35] on nanostructured systems. For example, Spinu *et al.*[34] observed a rounded peak around $H=0$ in the χ_T response of Co nanoparticles, dispersed in a wax matrix, when the system was below but close to the average blocking temperature. These results show that this sample is still ferromagnetic at room temperature but it is close to the superparamagnetic state. Finally, the sample with a Co nominal thickness of 10 nm and Au capping layer shows a χ_T curve different from the other. The expected peak at $-H_C$ is absent due to the anisotropy field dispersion, which produces the broadening of the peaks detected in the effective anisotropy field.[11] This broadening can mask the expected peak at $-H_C$. From the position of the peaks, we have obtained the effective anisotropy field ($H_{K,\text{eff}}$), which has been included in Table II.

It is important to mention that the drastic effect of the Pt capping layer has also been detected in the χ_T measurements, as can be seen in Fig. 6(b). In this case, the expected peaks in $\pm H_{K,\text{eff}}$ are always detected, even in the thinner samples. When the Co nominal thickness is increased, the peaks are more broadened and the position around $H=0$ becomes less symmetric. There is also an increase of the asymmetry in the peak heights. These features are related to the anisotropy field dispersion and the interparticle interaction. As was shown in the morphological studies, σ_D increases as t_{Co} increases, so σ_D exerts an influence on the anisotropy field dispersion. As a consequence, the magnetization reversal takes place in a wider range of magnetic-field values. Interparticle interaction is controlled by the distance between particles and the surface contact. In Fig. 6(c) we have plotted $H_{K,\text{eff}}$ vs D for the samples with $t_{\text{Co}}=2$, 3, and 5 nm, with Pt capping layer. Once more, the experimental data are closer to D^6 dependence, which is in agreement with the RAM for a 3D system. However, these $H_{K,\text{eff}}$ values are too low com-

Downloaded 28 Apr 2009 to 161.111.235.57. Redistribution subject to AIP license or copyright; see http://jap.aip.org/jap/copyright.jsp

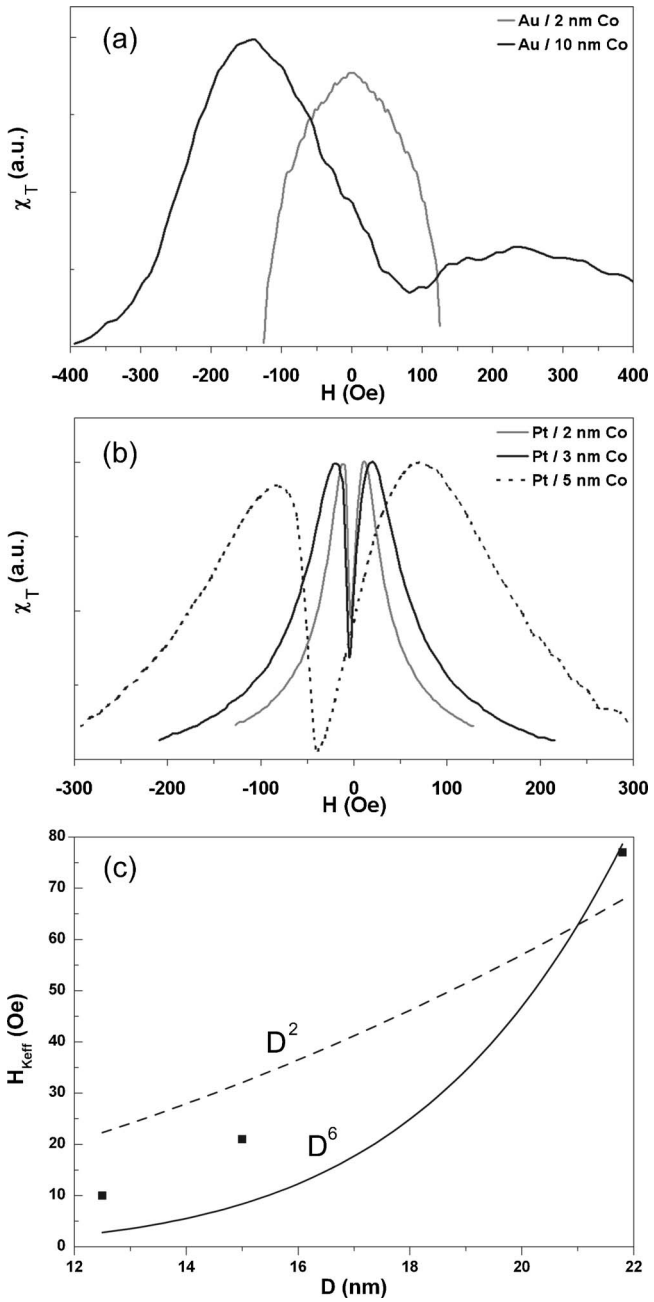

FIG. 6. (a) Transverse susceptibility for Au capped samples with Co nominal thicknesses of 2 and 10 nm. (b) Transverse susceptibility for Pt capped samples with Co nominal thicknesses of 2, 3, and 5 nm. (c) Dependence of Pt capped Co nanoparticles' effective anisotropy field on particle size with the corresponding fits to D^6 law (solid line) and D^2 law (dashed line).

pared to that of the effective anisotropy predicted by this model.[26] For example, for Co nanocrystalline particles with a correlation length of 4 nm, the RAM predicts an effective anisotropy field of 1600 Oe. Therefore we have to take into account the effect of the relaxation of the particle magnetic moments. In our case, the α values are lower for the thinner samples (see Table II), so the thermal energies will affect the effective anisotropy observed at room temperature. When the Co nominal thickness is increased, the activation energy increases, showing a higher effective anisotropy field. This implies that the Pt capped samples with $t_{Co}=10$ and 15 nm have enough activation energy so that the peaks in the χ_T are detected closer to the anisotropy field of bulk Co. That is the

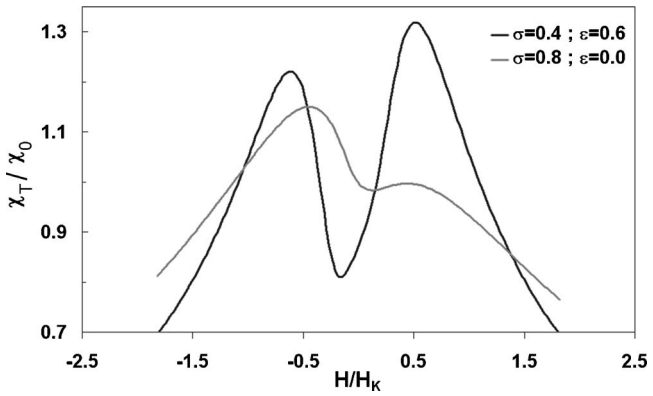

FIG. 7. Theoretically determined χ_T plots for a randomly oriented nanoparticle system with two different values of the anisotropy field dispersion (σ) and interparticle interaction (ε) according to the model described in Ref. 13.

reason why they were not detected with the magnetic fields attained in our experiment. This behavior in the χ_T measurements is similar to that obtained by Spinu *et al.*[14,15] by varying the temperature in magnetic nanoparticle systems of Fe and γ-Fe_2O_3. The idea is the same, so a change of the magnetic volume or the temperature leads to a change of the parameter α.

It is worth mentioning that valuable information can be obtained from a close study of the shape of the peaks of χ_T curves. Let us compare χ_T for the Pt capped, 5 nm Co sample with χ_T for the Au capped, 10 nm Co sample. First of all, while the peak at $H=H_{K,\text{eff}}$ is higher than the peak at $H=-H_{K,\text{eff}}$ for the Pt capped sample, the reversed is observed in the case of the Au capped one [see Figs. 6(a) and 6(b)]. Secondly, the peaks of the Au capped sample are more broadened than those of the Pt capped one due to a higher anisotropy dispersion in the former sample. This can be attributed to the fact that the particle size dispersion has more than doubled when the Co nominal thickness is increased from 5 to 10 nm, as can be seen in Table I. All these features can be qualitatively explained by a theoretical model described elsewhere.[13] In this model, the effects on the χ_T of the anisotropy field dispersion (σ), interparticle interaction (ε), and texture (σ_ϕ and σ_θ) have been studied. In Fig. 7, we have calculated the χ_T for a randomly oriented nanoparticle system with two different values of σ and ε. In the first case, a system with strong interparticle interaction ($\varepsilon=0.6$), representing the case of Pt/Co thin film, is considered. In the second case, the χ_T is calculated without interparticle interaction ($\varepsilon=0$) and with twice the anisotropy field dispersion, representing the case of Au/Co thin film, in agreement with the change of ε and σ from one sample to the other. The correlation between experimental and theoretical χ_T data shows two important features. On the one hand, the anisotropy field dispersion is intrinsically related to the particle size dispersion. On the other hand, the interparticle interaction can be strongly modified by the capping layer. A highly polarizable capping layer (like Pt) can connect magnetically the Co nanoparticles, promoting an increase of the effective magnetic volume, and so be used for decreasing the blocking temperature of a nanostructured system. However, a low polarizable capping layer (like Au) does not produce a magnetic connection among nanoparticles. That is the reason

Downloaded 28 Apr 2009 to 161.111.235.57. Redistribution subject to AIP license or copyright; see http://jap.aip.org/jap/copyright.jsp

why the sample Au/2 nm Co tends to the superparamagnetic state, whereas the sample Pt/2 nm Co exhibits a clear effective anisotropy field.

IV. CONCLUSIONS

We have presented a study on the properties of Co nanoparticles grown on Si_3N_4. The system has a clear 3D growth due to the high temperature of the substrate during deposition. For nominal thicknesses up to 5 nm, Co nanoparticles exhibit a narrow distribution of sizes. However, the percolation between nanoparticles occurs for thicker samples, giving rise to an increase in the particle size distribution. We have shown that the effective magnetic anisotropy depends dramatically on the particle size, the distribution of sizes, and the magnetic interaction among the nanoparticles. The interparticle interaction can be controlled by the capping layer, so that when a highly polarizable material (Pt) is used, a strong magnetic interaction between the nanoparticles is observed. This can be used as a means of changing the effective magnetic anisotropy in nanostructured systems.

ACKNOWLEDGMENTS

This work was supported in part by Universidad de Oviedo. One of the authors (B.P.) gratefully thanks Dr. Luis Eugenio Fernandez-Outon and Dr. Gonzalo Vallejo-Fernandez for the support received in the particle size analysis. Also, B.P. acknowledges financial support received from Gobierno del Principado de Asturias under Grant No. BP05-015. J.M.G.M. wishes to thank the financial support from CSIC under Project No. PIE 200650 130. C.C. acknowledges the Ministerio de Educación y Ciencia and FPI program for financial support.

[1]S. Sun and C. B. Murray, J. Appl. Phys. **85**, 4325 (1999).
[2]V. F. Puntes, P. Gorostiza, D. M. Aruguete, N. G. Bastus, and A. P. Alivisatos, Nat. Mater. **3**, 263 (2004).
[3]S. Sun, C. B. Murray, D. Weller, L. Folks, and A. Moser, Science **287**, 1989 (2000).
[4]V. F. Puntes, K. M. Krishnan, and A. P. Alivisatos, Science **291**, 2115 (2001).
[5]C. G. Zimmermann, M. Yeadon, K. Nordlund, J. M. Gibson, R. S. Averback, U. Herr, and K. Samwer, Phys. Rev. Lett. **83**, 1163 (1999).
[6]C. D'Orléans *et al.*, Phys. Rev. B **67**, 220101(R) (2003).
[7]F. Tang, D.-L. Liu, D.-X. Ye, Y.-P. Zhao, T.-M. Lu, G.-C. Wang, and A. Vijayaraghavan, J. Appl. Phys. **93**, 4194 (2003).
[8]X. Du, M. Inokuchi, and N. Toshima, J. Magn. Magn. Mater. **299**, 21 (2006).
[9]Y. Shiratsuchi, M. Yamamoto, Y. Endo, D. Li, and S. D. Bader, J. Appl. Phys. **94**, 7675 (2003).
[10]F. Luis *et al.*, Phys. Rev. B **65**, 094409 (2002).
[11]A. Hoare, R. W. Chantrell, W. Schmitt, and A. Eiling, J. Phys. D **26**, 461 (1993).
[12]L. Spinu *et al.*, Appl. Phys. Lett. **86**, 012506 (2005).
[13]R. Matarranz, M. C. Contreras, G. Pan, B. Presa, J. A. Corrales, and J. F. Calleja, J. Appl. Phys. **99**, 08Q504 (2006).
[14]L. Spinu, H. Srikanth, E. E. Carpenter, and C. J. O'Connor, J. Appl. Phys. **87**, 5490 (2000).
[15]L. Spinu, H. Srikanth, J. A. Wiemann, S. Li, J. Tang, and C. J. O'Connor, IEEE Trans. Magn. **36**, 3032 (2000).
[16]F. Luis *et al.*, J. Appl. Phys. **99**, 08G705 (2006).
[17]M. Suzuki *et al.*, Phys. Rev. B **72**, 054430 (2005).
[18]C. Train, P. Beauvillain, V. Mathet, G. Pénissard, and P. Veillet, J. Appl. Phys. **86**, 3165 (1999).
[19]Y. P. Lee, K. W. Kim, R. Gontarz, and Y. V. Kudryavtsev, Curr. Appl. Phys. **1**, 451 (2001).
[20]F. Wilhelm *et al.*, Phys. Rev. B **69**, 220404(R) (2004).
[21]M. Vopsaroiu, G. Vallejo Fernandez, M. J. Thwaites, J. Anguita, P. J. Grundy, and K. O'Grady, J. Phys. D **38**, 490 (2005).
[22]Nanotec Electronica SL™, www.nanotec.es
[23]J. Arbiol, F. Peiró, A. Cornet, C. Clavero, A. Cebollada, G. Armelles, and Y. Huttel, Appl. Phys. Lett. **86**, 032510 (2005).
[24]R. C. O'Handley, *Modern Magnetic Materials: Principles and Applications* (Wiley, New York, 2000).
[25]S. H. Charap, P. L. Lu, and Y. He, IEEE Trans. Magn. **33**, 978 (1997).
[26]G. Herzer, Mater. Sci. Eng., A **133**, 1 (1991).
[27]A. Kharmouche, S.-M. Chérif, A. Bourzami, A. Layadi, and G. Shmerber, J. Phys. D **37**, 2583 (2004).
[28]A. Aharoni, E. H. Frei, S. Shtrikman, and D. Treves, Bull. Res. Counc. Isr., Sect. A: Math., Phys. Chem. **6**, 215 (1957).
[29]L. Pareti and G. Turilli, J. Appl. Phys. **61**, 5098 (1987).
[30]Ch.-R. Chang and J.-S. Yang, Appl. Phys. Lett. **65**, 496 (1994).
[31]L. Spinu, C. J. O'Connor, and H. Srikanth, IEEE Trans. Magn. **37**, 2188 (2001).
[32]L. Spinu, C. Cimpoesu, L. Stoleriu, and A. Stancu, IEEE Trans. Magn. **39**, 2516 (2003).
[33]P. Poddar, H. Srikanth, S. A. Morrison, and E. E. Carpenter, J. Magn. Magn. Mater. **288**, 443 (2005).
[34]L. Spinu, Al. Stancu, L. D. Tung, J. Fang, P. Postolache, H. Srikanth, and C. J. O'Connor, J. Magn. Magn. Mater. **242–245**, 604 (2002).
[35]J. F. Calleja, M. C. Contreras, R. Matarranz, E. Navarro, Y. Huttel, A. Cebollada, and G. Armelles, J. Appl. Phys. **97**, 104302 (2005).

Downloaded 28 Apr 2009 to 161.111.235.57. Redistribution subject to AIP license or copyright; see http://jap.aip.org/jap/copyright.jsp